

# EEG motor imagery decoding: A framework for comparative analysis with channel attention mechanisms

Martin Wimpff<sup>1</sup>, Leonardo Gizzi<sup>2</sup>, Jan Zerfowski<sup>3</sup>, Bin Yang<sup>1</sup>

<sup>1</sup>Institute of Signal Processing and System Theory, University of Stuttgart, Germany

<sup>2</sup>Fraunhofer Institute for Manufacturing Engineering and Automation IPA, Germany

<sup>3</sup>Clinical Neurotechnology Laboratory, Department of Psychiatry and Neurosciences, Charité Campus Mitte (CCM), Charité - Universitätsmedizin Berlin, Germany

E-mail: martin.wimpff@iss.uni-stuttgart.de

**Abstract.** *Objective* The objective of this study is to investigate the application of various channel attention mechanisms within the domain of brain-computer interface (BCI) for motor imagery decoding. Channel attention mechanisms can be seen as a powerful evolution of spatial filters traditionally used for motor imagery decoding. This study systematically compares such mechanisms by integrating them into a lightweight architecture framework to evaluate their impact. *Approach* We carefully construct a straightforward and lightweight baseline architecture designed to seamlessly integrate different channel attention mechanisms. This approach is contrary to previous works which only investigate one attention mechanism and usually build a very complex, sometimes nested architecture. Our framework allows us to evaluate and compare the impact of different attention mechanisms under the same circumstances. The easy integration of different channel attention mechanisms as well as the low computational complexity enables us to conduct a wide range of experiments on three datasets to thoroughly assess the effectiveness of the baseline model and the attention mechanisms. *Results* Our experiments demonstrate the strength and generalizability of our architecture framework as well as how channel attention mechanisms can improve the performance while maintaining the small memory footprint and low computational complexity of our baseline architecture. *Significance* Our architecture emphasizes simplicity, offering easy integration of channel attention mechanisms, while maintaining a high degree of generalizability across datasets, making it a versatile and efficient solution for EEG motor imagery decoding within brain-computer interfaces.

## 1. Introduction

In the field of modern neuroscience and technology, researchers and clinicians are exploring innovative approaches to bridge the gap between the human brain and external devices. One avenue of research is electroencephalogram (EEG) motor imagery decoding, which holds great promise for improving neurorehabilitation strategies. EEG has emerged as a key technology for deciphering the intricate relationship between the mind and bodily movements because it is a non-invasive, versatile and affordable

technique for measuring brain activity. Motor imagery, the mental simulation of movement without actual execution, generates EEG patterns similar to those generated during actual execution. These patterns can be decoded and translated into meaningful commands, enabling direct communication between the brain and external devices. Brain-computer-interfaces (BCIs), based on the principles of EEG motor imagery decoding, provide a pathway for individuals with motor impairments to regain lost functionality. Such interfaces offer unprecedented opportunities for people with conditions like spinal cord injuries, stroke or neurodegenerative diseases to restore a degree of independence and improve their quality of life. One critical aspect of BCIs is the decoding algorithm used to translate the measured brain activity into meaningful commands. Our work is centered on understanding and investigating different deep learning solutions for the decoding problem.

Since the introduction of AlexNet in 2012, deep neural networks (DNN) have transformed many fields including computer vision, natural language processing and medicine. Throughout the years, the underlying architectures became bigger, wider and deeper to solve increasingly complex tasks at the level of a human and beyond. Currently, generative pre-trained transformer (GPT) models like ChatGPT as well as vision transformers are creating a new hype around the role of attention and especially around the transformer architecture. While the attention mechanism and transformers are well understood and investigated in the natural language processing and computer vision area, attention is still largely unexplored in the context of BCI and EEG.

[1, 2, 3, 4, 5, 6] all use a squeeze-and-excitation (SE) module in their architecture. [1] builds a complex hybrid architecture with common spatial patterns (CSP), SincNet filters, an SE module, temporal and spatial convolutions as well as gated recurrent units (GRU). [2] created a feature fusion model that uses the SE block to combine deep and multi-spectral features. [3, 4] created multi-branch convolutional neural networks (CNN) in combination with SE modules. The architecture by [4] additionally involves an Inception-Block [7] and a ResNet [8]. [5] and [6] use time-frequency representations instead of raw time series.

[9, 10, 11, 12, 13, 14, 15, 16, 17] use other types of attention mechanisms. [9] uses an inception-like CNN together with a kind of attention that is not described further. We believe that it is something within the category of multi-head self-attention (MHSA) [18]. [10] built an architecture consisting of a convolutional stage as in ShallowNet [19] and EEGNet [20] followed by MHSA blocks attending over the temporal direction. [11] uses a similar convolutional stage followed by an ensemble of blocks consisting of MHSA and temporal convolutional blocks [12]. [13] on the other hand uses a graph-based CNN together with a recurrent attention module composed of long short-term memory cells (LSTM). [14] uses a complex time-distributed attention architecture, where the EEG signal is initially split into non-overlapping segments and further spatially filtered. Afterwards, the segments get classified through parallel attention modules (one for each segment) followed by an LSTM and a fully connected layer.

Further, there are some works that combine different attention mechanisms like

[15, 16, 17]. [15] combines a custom lightweight channel recalibration module with the channel attention module from ECA-Net [21]. [16] combines a channel attention module based on the wavelet packet sub-band energy ratio with a temporal attention mechanism followed by a feature fusion architecture. [17] builds a model for emotion recognition that also uses a form of channel-wise attention together with LSTMs and self-attention. We observed that while there is a number of publications about EEG-based BCI using attention, most of them use very complex and task-specific, computationally inefficient, hybrid/multi-branch/multi-scale/ensemble/time-distributed architectures and all of them investigate only one attention mechanism. The two time-frequency solutions [5, 6] as well as the EEGConformer [10] are an exception by having a simple, non-nested architecture.

The insights learned from such specialized and narrow investigations as well as the ability to transfer these learnings to other problems is often limited. An additional problem with complex architectures is their computational complexity as well as comparability. Different models are difficult to compare as each of them uses different layers before and after the layers with attention as well as a different training routine. Those are all reasons that lead to high entry barriers, confusion and mistrust by medical experts towards the deployment of deep learning in BCI. Hence, most of the experts still rely on classical algorithms like CSP [22, 23] or on the somewhat outdated but well explored shallow architectures EEGNet or ShallowNet.

To overcome these limitations, we first introduce a simple yet powerful baseline model without any attention mechanism. We will also showcase the process of how we developed this baseline architecture from the well-known EEGNet and ShallowNet to justify our design choices. We then integrate different channel attention mechanisms into this architecture framework while keeping the network and training routine constant across all experiments to allow for a fair comparison. This allows us to measure the real impact and suitability of each attention mechanism. We believe that this fair and systematic comparison is able to increase the understanding of attention in BCIs. Moreover, it serves as a foundational platform for forthcoming research in the realms of attention in BCI. The source code is available at <https://github.com/martinwimpff/channel-attention> and was developed using the python packages pytorch [24], pytorch-lightning [25], braindecode [19], mne-python [26] and moabb [27].

## 2. Method

### 2.1. Task and dataset

As a dataset we will mainly use the BCI competition IV 2a dataset provided by the University of Graz [28] as it is the most popular EEG motor imagery dataset. The study consists of EEG data from 9 subjects recorded on 22 electrodes at 250 Hz imagining one of four different classes (feet, left hand, right hand and tongue movement) per trial. The

data was acquired in two sessions recorded on different days with 288 trials per session and subject. Each trial has an imagination period of four seconds, where the visual cue (an arrow pointing down, left, right or up) is present for the first 1.25s of imagination. In our experiments we will use the full four seconds at the original 250 Hz. We train one model per subject and use the data from the first session for training while the data of the same subject from the second session will be used for testing. We are not performing experiments across different subjects since the existing reference methods are not optimized for such situations. This is primarily due to the significant variability observed among subjects, necessitating the adoption of transfer learning techniques to effectively address the inherent inter-subject differences.

To investigate the transferability of our observations, we additionally conduct some experiments on the BCI competition IV 2b dataset [29] and the High Gamma dataset (HGD) [19]. Similar to the 2a dataset, the 2b dataset also involves 9 subjects and is recorded at 250 Hz. The main differences are that it uses only three electrodes and only distinguishes between two different classes (left hand and right hand). Additionally, the trials last 4.5s instead of 4s and the data was recorded in 5 sessions of which the first three (400 trials) will be used for training and the last two (320 trials) will be used for testing.

The HGD is the biggest dataset and has EEG data from 14 subjects recorded at 250 Hz on 128 electrodes of which only 44 sensors covering the motor cortex are used. Similar to the 2a dataset, the trials lasted 4s and four different movements (left hand, right hand, feet, rest) were imagined. The training data consists of approx. 880 trials per subject and the test data of approx. 160 trials per subject.

## 2.2. BaseNet

Previous publications [19, 20, 2, 3, 10, 11, 12] working on EEG motor imagery decoding have shown that it is helpful to use a stem-block as a first layer of the architecture. This block is usually composed of a temporal convolutional layer and a spatial convolutional layer along with normalization layers, nonlinearity and pooling layers. Since EEGNet and ShallowNet, most of the successive deep learning architectures used a somewhat similar approach. The problem, however, is that every publication tends to use a slightly different stem-block, some are closer to the one used in ShallowNet, some are more similar to the one in EEGNet. Different kernel sizes, number of filters, normalizations, nonlinearities, pooling layers and weight initializations between different architectures impair the comparability as it is not clear to which part of the network a possible improvement can be attributed to. Moreover, comparing a very complex and specialized architecture to a somewhat dated architecture like EEGNet or ShallowNet without adjusting the hyperparameters and training routine raises concerns about the validity of the comparison. To overcome this limitation, we decided to develop a unified shallow neural network called BaseNet, which aims to be parameter-efficient and expressive with plausible and simple hyperparameter choices. To do so, we gradually combined,

simplified and modernized the design choices from EEGNet and ShallowNet to create a strong baseline model. The architecture is visualized in Figure 2a.

The first step is the simplification of the training routine. We use the full 4s trial at 250 Hz instead of a shortened trial at a lower sampling frequency to provide the full original information to the network. Further, we train the model for a fixed number of epochs (1000) using a learning rate scheduler with a linear warmup of 20 epochs followed by a cosine decay instead of using early stopping to reduce loss oscillations while avoiding an additional data split.

The second step involves the simplification of the architecture. To simplify, we use a linear classification layer and always use the default initialization and batch normalization of pytorch. Further, our model does not use bias in the convolutional layers and does not use any kernel weight constraints. We use the grouped convolutions from EEGNet as well as their intermediate batch normalization layer between the first two layers to reduce the number of parameters and to regularize the training.

The next step involves the choice of activation function, kernel sizes and pool sizes. We chose the ELU activation function from EEGNet instead of the square-log function from ShallowNet as it resulted in better performance. We used the kernel and pool sizes of ShallowNet as it was originally developed for trials at 250 Hz in contrast to EEGNet, which was developed for trials at 128 Hz. We chose to use the depthwise separable convolution from EEGNet to add depth to the model while keeping a low memory footprint. To decouple the channel dimension in the spatial layer from the channel dimension in the depthwise separable convolution, we further added a  $1 \times 1$  convolutional channel projection layer as in EEGConformer [10]. We then used the filter sizes from EEGNet for the depthwise separable convolution and the filter sizes from ShallowNet for the first two convolutional layers.

To investigate the use of the different channel attention mechanisms, the attention mechanisms introduced in the next section have to be integrated into the BaseNet architecture. We do this by simply adding the channel attention block between the nonlinearity of the depthwise separable convolution and the pooling layer. This position is visualized by a red dot in Figure 2a.

### 2.3. Attention

Attention enables humans to selectively process and prioritize information from a multitude of sensory stimuli, focusing on those that are relevant to specific goals and cognitive processes. The deep learning community has tried to include different kinds of attention mechanisms for many years (see [30] for a review). The different attention mechanisms can be macroscopically categorized by the domain they are operating in. [30] distinguishes between channel, spatial, temporal and branch attention as well as combinations where the attention mechanism operates on two domains.

The success and wide use of spatial filters for motor imagery decoding highlights the importance of the spatial distribution of brain activity. The areas of interest for

motor imagery decoding (namely, the motor and sensory cortices) are somatotopically organized, and different cortical areas can be associated with different functions or areas of the body. We will therefore focus on the spatial dimension and compare different channel attention mechanisms in this paper. As EEG data and images have different dimensions, we first want to clarify the terms "spatial" and "channel" to avoid further confusion.

EEG data typically consists of multiple time series (temporal dimension) from different sensors (spatial dimension) and can be described by a tensor  $X_{\text{eeg}} \in \mathbb{R}^{C \times T}$  where  $C$  is the number of EEG sensors and  $T$  is the number of time points. Images, on the other hand, are three-dimensional tensors  $X_{\text{img}} \in \mathbb{R}^{C \times H \times W}$  where  $C$  describes the number of color channels of the input image and later the number of feature channels of intermediate tensors,  $H$  the height and  $W$  the width. As we investigate the use of channel attention mechanisms originating from the image domain for EEG data, the dimension of the color channels  $C$  from images  $X_{\text{img}}$  corresponds to the spatial dimension ( $C$ ) of the EEG tensor  $X_{\text{eeg}}$ . We also examine two architectures with additional attention in the spatial domain in images ( $H$  and  $W$ ) which transfers to the temporal domain  $T$  in EEG data. It is worth noting that the attention mechanisms attend over feature channels rather than EEG channels as the second layer (spatial convolution) as well as the channel projector already filter the original input spatially. This is similar to images where the color channels become feature channels after the first convolutional layer. In the following sections we will only use the terms "channel" and "temporal" for clarity.

*2.3.1. General form* The general process of attending to a specific region can be formulated as

$$\text{Attention} = f(a(x), x) \quad (1)$$

where  $a(x)$  represents the function that generates the attention.  $f(a(x), x)$  means that the input  $x$  is processed based on the attention generated by  $a(x)$  (cf. [30]). This general form allows us to describe different attention mechanisms in a unified manner.

*2.3.2. Squeeze-and-excitation* Squeeze-and-excitation network (SENet) [31] is a simple yet powerful way to enhance feature representations by adaptively re-calibrating channel-wise information. SENet can be seen as the pioneer of channel attention on which most of the subsequent works are founded. It can be formulated as

$$a(x) = \sigma(\text{MLP}(\text{GAP}(x))) = \sigma(W_2 \phi(W_1 \text{GAP}(x))) \quad (2)$$

$$f(a(x), x) = a(x) \otimes x \quad (3)$$

where global average pooling (GAP) calculates the average of  $T$  samples for each channel ( $\mathbb{R}^{C \times T} \rightarrow \mathbb{R}^C$ ) and the multi-layer-perceptron (MLP) learns adaptive attention weights ( $\in \mathbb{R}^C$ ) per channel. The MLP consists of two fully connected Layers (FC) connected by a ReLU activation function ( $\phi$ ) to enable nonlinearity. The first FC projects the channel dimension  $C$  to a lower dimension  $C' = C/r$  by multiplying with  $W_1 \in \mathbb{R}^{C' \times C}$ ,

where  $r \geq 1$  is called the reduction rate. The second FC projects the attention weights back to the initial channel dimension  $C$  by multiplying with  $W_2 \in \mathbb{R}^{C \times C'}$  followed by a sigmoid activation function  $\sigma$  mapping each value to a range between 0 and 1. Finally, each channel of the original input  $x$  gets multiplied elementwise by  $a(x)$ . The GAP layer represents the squeeze module, whereas the excitation module comprises of the MLP and the sigmoid function. The SE block is visualized in Figure 1a. The following channel attention mechanisms try to improve the SE block in different ways. We arranged the following sections based on the improved part of SE. All channel attention mechanisms studied in this paper are visualized in Figure 1.

*2.3.3. Improving the squeeze module* [32, 33, 34] try to improve the original SE module by changing the squeeze module which is a GAP layer in SE to something more expressive. [32] argue that a GAP layer is limited because it only calculates first-order statistics. Therefore they introduce a global second-order pooling (GSoP) block to model second-order statistics. Mathematically, the attention part of a GSoP block is given by

$$a(x) = \sigma(\text{FC}(\text{RwConv}(\text{Cov}(\text{Conv}(x)))))) \quad (4)$$

The initial  $1 \times 1$  convolution reduces the number of channels  $C$  to  $C'$ . Afterwards, a  $C' \times C'$  covariance matrix is computed. Subsequently, a row-wise normalization is performed through a row-wise convolution which results in a one dimensional feature vector  $\in \mathbb{R}^{C'}$ . The fully-connected layer as well as the sigmoid function is similar to SE. [33], on the other hand, view the squeeze module as a compression problem and use the discrete cosine transform (DCT) to decompose the features in the frequency domain. The GAP layer of SE is replaced by a grouped DCT module that divides the original input with  $C$  channels into  $n_{groups}$  groups with each  $C' = C/n_{groups}$  channels and then multiplies each group of channels element-wise with different DCT bases corresponding to different frequencies.  $\text{DCT}^0$  is the DCT base with lowest frequency component and is equivalent to a scaled GAP layer (cf. [33] for mathematical derivation). The MLP and the sigmoid function stay the same as in SE. Formally, the attention of their Frequency Channel Attention Network (FCA) can be formulated as

$$a(x) = \sigma(\text{MLP}(\text{DCT}(\text{Group}(x)))) \quad (5)$$

[34] proposed a method particularly suited to semantic segmentation. Their attention mechanism has  $K$  learnable codewords or visual centers  $d_i \in \mathbb{R}^C$  with corresponding learnable smoothing factors  $s_i \in \mathbb{R}$ . Soft-assignment weights  $e_k = \sum_{i=1}^T e_{ik}$  are calculated with

$$e_{ik} = \frac{\exp(-s_k \|r_{ik}\|^2)}{\sum_{j=1}^K \exp(-s_j \|r_{ij}\|^2)} r_{ik}, \quad r_{ik} = x_i - d_k, \quad x_i \in \mathbb{R}^C \quad (6)$$

The soft-assignment weights are further aggregated by  $e = \sum_{k=1}^K \phi(e_k)$  where  $\phi$  represents a batch normalization and a ReLU activation function. The final attention function is then given by  $a(e) = \sigma(\text{FC}(e))$ . They additionally use a second loss function

especially tailored for semantic segmentation which we will not use, as we don't do semantic segmentation and only have one class per trial.

*2.3.4. Improving the excitation module* The ECA-Net [21] is the only method in this comparison that solely relies on improving the excitation module. In the original SE module the excitation module consists of two FC layers with  $C^2/r$  parameters each. To reduce the number of parameters, they proposed a method called local cross-channel attention that tries to balance the trade-off between cross-channel interaction and parameter efficiency by using a 1D convolution in the channel dimension after the GAP layer. The attention mechanism of ECA-Net can be formulated as

$$a(x) = \sigma(\text{Conv1D}(\text{GAP}(x))) \quad (7)$$

which only needs  $k$  parameters where  $k$  is the kernel size of the 1D convolution.

*2.3.5. Improving the squeeze and the excitation module* An early follow-up by the original authors called gather-excite (GE) [35] investigated the parameterization of the squeeze and the deparameterization of the excitation module. Originally, the squeeze module (GAP layer) has zero parameters. GE proposes a gather module that gathers information through a grouped convolution with a variable extent. If the kernel size  $k$  equals the length of the sequence ( $k = T$ ), the extent is called global. A global gather module introduces  $Ck = CT$  new parameters. They further investigate a parameter-free excitation module that simply scales each channel based on the sigmoid of its average value without any MLP ( $a(x) = \sigma(\text{GAP}(x))$ ).

Another method trying to reduce the number of parameters is the gated channel transformation (GCT) [36]. This method aggregates channel information by computing the  $l_2$ -norm per channel instead of the average. There are three learnable parameters  $\alpha_c, \beta_c$  and  $\gamma_c$  per channel  $c$  controlling the gating mechanism. Instead of a sigmoid function, tanh is used. GCT is given by

$$s_c = \alpha_c \cdot \|x_c\|_2, \quad \hat{s}_c = \frac{\sqrt{C}s_c}{[(\sum_{c=1}^C s_c^2) + \epsilon]^{\frac{1}{2}}}, \quad \epsilon = 10^{-5} \quad (8)$$

$$a(x) = 1 + \tanh(\gamma\hat{s} + \beta) \quad (9)$$

which reduces the number of parameters from  $2C^2/r$  (SENet) to  $3C$ .

While the previous approaches (except the parameter-free version from GE) all rely on cross-channel interaction, the style-based recalibration module (SRM) [37] investigates a channel-independent attention mechanism. They first collect  $d = 2$  style features (average and standard deviation) per channel, which they call style pooling. The following step is called style integration which linearly combines the style features per channel through a channel-wise fully connected (CFC) layer. The attention mechanism can be formulated by

$$a(x) = \sigma(\text{BN}(\text{CFC}(\text{Concat}([\text{GAP}(x), \text{STD}(x)])))) \quad (10)$$

where BN is a batch normalization layer and the CFC layer has  $dC$  learnable parameters.



2.3.6. *Channel and temporal attention mechanisms* SENet and the subsequent approaches used the attention mechanism only in the channel domain. However, there are combinations which attend over the temporal and channel domain.

The pioneering work for combining both types of attention is the convolutional block attention module (CBAM) [38]. CBAM is divided into a channel attention module and a temporal attention module. The channel attention module is almost similar to SENet and the attention mechanism is given by

$$a_{ch}(x) = \sigma(\text{MLP}(\text{GAP}(x)) + \text{MLP}(\text{GMP}(x))) \in \mathbb{R}^C \quad (11)$$

where the MLP is shared and the only difference to SENet is the additional (parameter-free) global max pooling (GMP) layer. Afterwards, nearly the same process is repeated in the temporal domain:

$$a_{temp}(x) = \sigma(\text{Conv2D}(\text{Concat}([\text{GAP}(x), \text{GMP}(x)]))) \in \mathbb{R}^T \quad (12)$$

The GAP and GMP layer now calculate the average and the maximum respectively over all channels, resulting in a concatenated feature map  $f \in \mathbb{R}^{2 \times T}$ . This feature map is then processed by a 2D convolutional layer resulting in a temporal attention map  $a_{temp}(x) \in \mathbb{R}^T$ . The complete attention mechanism of CBAM is given by

$$f(x, a_{ch}(x), a_{temp}(x)) = a_{temp}(a_{ch}(x) \otimes x) \otimes (a_{ch}(x) \otimes x) \quad (13)$$

While the temporal and channel attention module in CBAM do not cooperate explicitly, [39] introduced a mechanism called CAT specifically designed to allow collaboration between the two types of attention. In addition to the GAP and GMP layer in CBAM, they use a global entropy layer (GEP). Instead of concatenating the different feature maps, they use a weighted sum to get one feature map per direction of attention

$$C'_A = C_\alpha \text{MLP}(\text{GAP}(x)) + C_\beta \text{MLP}(\text{GMP}(x)) + C_\gamma \text{MLP}(\text{GEP}(x)) \quad (14)$$

$$T'_A = \text{Conv2D}(T_\alpha \text{GAP}(x) + T_\beta \text{GMP}(x) + T_\gamma \text{GEP}(x)) \quad (15)$$

where the parameters  $C_{\alpha/\beta/\gamma}, T_{\alpha/\beta/\gamma} \in \mathbb{R}$  control the collaboration between the aggregated features in the channel attention and temporal attention respectively. The final attention mechanism is then given by

$$a(x) = \sigma(C_W \cdot C'_A) + \sigma(T_W \cdot T'_A), \quad f(x, a(x)) = a(x) \otimes x \quad (16)$$

where  $C_W, T_W \in \mathbb{R}$  control the collaboration between the channel and temporal attention. To investigate the use of collaboration weights for channel attention without temporal attention, we propose a modified version of CAT which we call CATLite. The attention mechanism of CATLite is given by  $a(x) = C'_A$ .

## 2.4. Training

We train all of our models with the same training routine for each subject. To preprocess the EEG data, we use a 40 Hz lowpass filter for the BCI competition datasets and a 4 Hz highpass filter for the High Gamma dataset. For the other models we used the

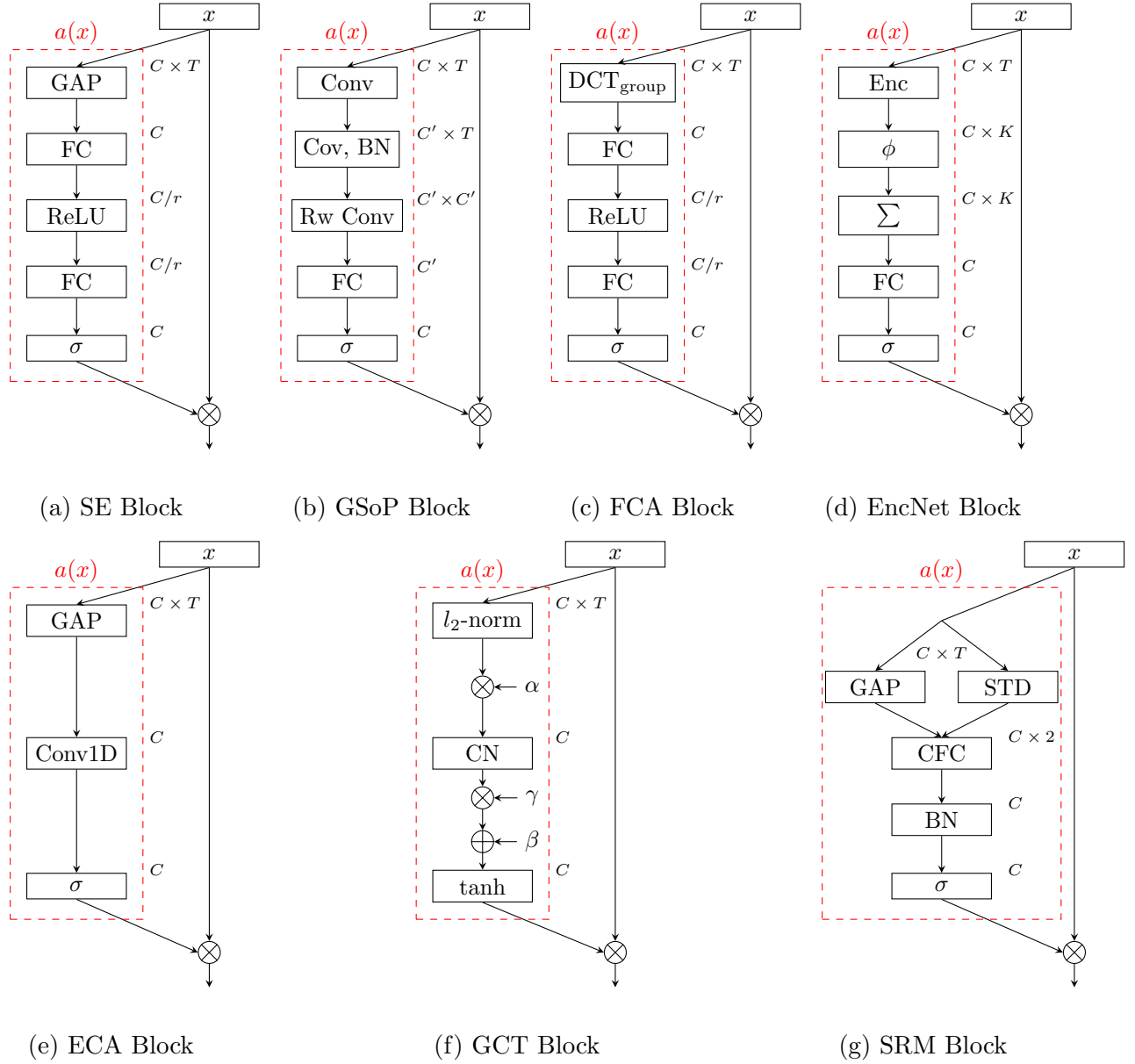


Figure 1: Channel attention mechanisms. GAP = global average pooling, FC = fully-connected layer, Cov=covariance pooling, BN=batch normalization, RW Conv = row-wise convolution,  $DCT_{\text{group}}$ =grouped discrete cosine transform, Enc=encoder block, CN=channel normalization, STD = global standard deviation, CFC= channel-wise fully-connected layer. Adapted from [30].

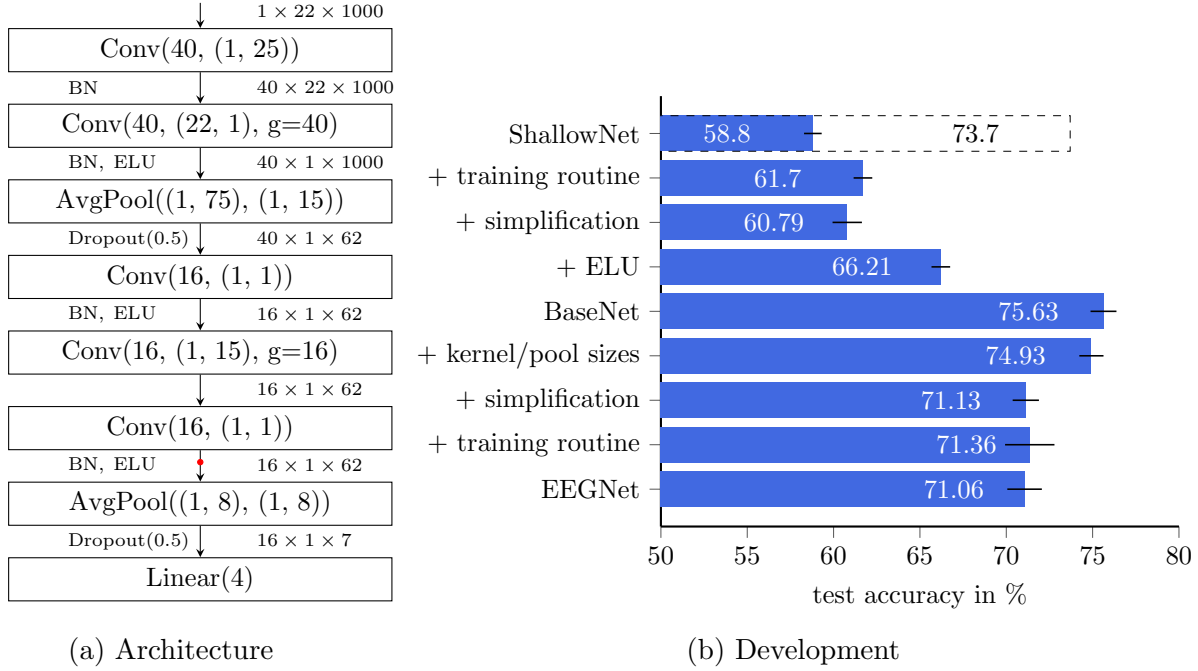


Figure 2: Architecture and development of BaseNet. (a):  $g$  = number of groups, BN = batch normalization. The red dot indicates the position of the optional channel attention mechanism. (b): The dashed bar represents the reported accuracy of ShallowNet with their cropped training strategy. The black error bars indicate the standard deviation for five runs with different random seeds.

filters they reported for the BCI competition datasets while we kept the 4 Hz highpass filter for all experiments with the HGD. We further normalize each channel to have zero mean and unit deviation. We then train all models for a fixed number of 1000 epochs and optimize via the Adam optimizer [40] with a learning rate of  $10^{-3}$ . We further use a learning rate scheduler with a linear warmup of 20 epochs followed by a cosine decay to reduce oscillations of the loss.

The test accuracy is evaluated on the last checkpoint. Each experiment is conducted five times with five different random seeds. The reported average accuracy is the average of these five runs. The reported standard deviation is the standard deviation of the average test accuracy (over all 9 subjects) between these five runs. This is done because the training process still involves a fair amount of randomness as the datasets are small and noisy and the dropout rate is very high (50%).

### 3. Results

The development of BaseNet from ShallowNet and EEGNet is visualized in Figure 2b. Developing BaseNet from ShallowNet, the introduction of the ELU function as well as the introduction of the depthwise separable convolution block along with the

Table 1: Results of all tested models in their best configuration. All results except ShallowNet\* were produced by us.

model	configuration	parameters	test acc. (%)
EEGNet	-	1.716	$71,06 \pm 1,0$
ShallowNet	-	44.644	$58,8 \pm 0,51$
ShallowNet*	cropped training	44.644	<b>73,7</b>
BaseNet	-	3.692	$75,63 \pm 0,75$
<b>BaseNet + SE</b>	r=4	3.820	<b><math>76,9 \pm 0,61</math></b>
BaseNet + GSoP	r=4	4.120	$76,28 \pm 1,05$
BaseNet + FCA	DCT <sup>0</sup>	4.812	$76,33 \pm 0,82$
BaseNet + EncNet	4 codewords	4.040	$76,37 \pm 0,76$
<b>BaseNet + ECANet</b>	k=9	3.695	<b><math>76,86 \pm 0,63</math></b>
BaseNet + GE- $\theta^-$	-	3.692	$75,57 \pm 0,35$
BaseNet + GE- $\theta$	e=global	4.716	$75,69 \pm 0,84$
BaseNet + GE- $\theta^+$	e=global, r=4	4.844	$74,95 \pm 0,87$
BaseNet + GCT	-	3.740	$75,96 \pm 1,04$
BaseNet + GCT <sub>GAP</sub>	-	3.740	$75,92 \pm 0,82$
BaseNet + SE- $l_2$	r=4	3.820	$75,89 \pm 0,65$
BaseNet + SRM	-	3.756	$75,65 \pm 0,41$
BaseNet + SRM <sub>cross</sub>	r=2	4.492	$76,3 \pm 0,8$
BaseNet + CBAM	k=15, r=8	3.787	$76,75 \pm 0,65$
<b>BaseNet + CAT</b>	k=3, r=4	5.641	<b><math>76,88 \pm 1,05</math></b>
<b>BaseNet + CATLite</b>	r=4	3.848	<b><math>76,91 \pm 0,9</math></b>
TS-SEFFNet [2]	-	334.824	$73,5 \pm 0,42$
EEGConformer [10]	-	789.572	$75,79 \pm 0,26$
<b>ATCNet [11]</b>	-	113.732	<b><math>79,08 \pm 0,43</math></b>
EEGTCNet [12]	act=ELU	4.096	$75,62 \pm 0,66$

channel projector have the greatest impact on the performance. For the evolution from EEGNet to BaseNet on the other hand, changing the kernel and pool sizes shows the greatest impact. Developing BaseNet from ShallowNet and EEGNet, the performance improves with each design change except the simplification step. We therefore also ran experiments without this simplification step. The final performance however was worse, indicating that those specialized design choices only suit their original architectures and training routine but can easily be removed for BaseNet.

### 3.1. Channel attention mechanisms

Table 1 shows the results of all tested models on the BCI competition dataset 2a. The CATLite attention block yielded the best results of all models using channel attention. The simple SE module, the parameter-efficient ECANet, as well as CAT, resulted in

almost the same performance. Improving only the squeeze module (GSoP, FCA, EncNet) resulted in a performance degradation compared to SE, while there was still an improvement compared to BaseNet. For FCA, the single  $DCT^0$  component, which is similar to a scaled GAP layer, gave the best results. This indicates that the element-wise multiplication with DCT components is not a powerful channel compression strategy for EEG decoding.

Solutions improving the squeeze and the excitation module showed results around the level of BaseNet, with the cross-channel SRM version  $SRM_{cross}$  showing the best results.  $SRM_{cross}$  is a modification of SRM using a MLP (as in SE) instead of the channel-wise fully-connected layer to measure the importance of cross-channel interaction. The GE solutions all perform at or below the level of BaseNet, which indicates that the parameterization of the original SE module is superior. GCT resulted only in slightly better results than BaseNet, which might be a sign of two things: 1) GAP is more expressive than  $l_2$ -norm 2) the degree of channel-interaction in the GCT mechanism is not sufficient for the complex interrelationships between the channels. To investigate this, we introduced two modifications: GCT with a GAP layer instead of using  $l_2$ -norm ( $GCT_{GAP}$ ) and an SE module using the  $l_2$ -norm instead of GAP layer ( $SE-l_2$ ). As all three versions result in a similar performance, we suppose that both design choices have approximately the same influence.

CBAM and CAT both show good performance. However, despite their similarities, their best configuration differs. As Table 1 only shows the results of the best configuration, we also ran some ablation studies to measure the effect of the hyperparameters of the attention modules.

### 3.2. Ablations

The reduction rate  $r$  determines the number of parameters ( $2C^2/r$ ) of an SE module for a given number of channels  $C$ . We evaluated different reduction rates in Figure 3a. The results show that while  $r = 4$  yields the best results, all configurations surpass the performance of BaseNet which demonstrates the general usefulness of the SE-block. The investigation also shows that higher reduction rates work slightly better than lower reduction rates.

To investigate the degree of cross-channel interaction, we varied the kernel size of ECANet and present the results in Figure 3b. The results show that a medium sized kernel yields almost the same results as SENet, which uses global cross-channel interaction. Apart from that, it is difficult to deduce a valid rule from the results.

As CBAM and CAT both showed very good performance but their best configurations regarding the reduction ratio  $r$  and the kernel size  $k$  differed, we decided to investigate this relationship closer. Figure 4 shows that the best configuration of CAT ( $k = 3, r = 4$ ) is the worst configuration for CBAM. Apart from that, a large kernel size ( $k = 15$ ) together with a reduction ratio  $r > 1$  works well for both mechanisms.

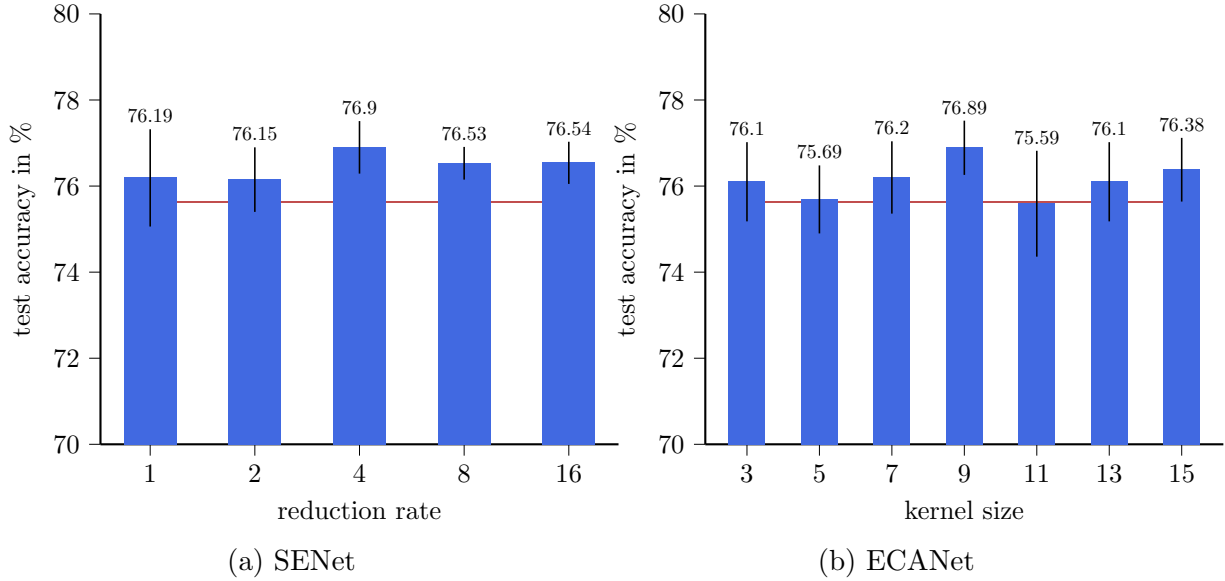


Figure 3: Ablation studies investigating the influence of the reduction rate and the kernel size for SENet and ECANet respectively. The red line indicates the average test accuracy of BaseNet.

Table 2: CATLite ablation results.

configuration	test acc. (%)
GAP + GMP + GEP	76,91 $\pm$ 0,9
GAP + GMP	76,77 $\pm$ 0,94
GAP + GEP	76,94 $\pm$ 0,84
GMP + GEP	76,88 $\pm$ 0,90
GAP	76,83 $\pm$ 0,94
GMP	76,87 $\pm$ 0,99
<b>GEP</b>	<b>77,01 <math>\pm</math> 0,93</b>

As CATLite involves three different channel features (average, maximum and entropy) instead of just the average in the SE module, we investigated the impact of these features on the final performance. To do so, we checked every possible combination of the three features which resulted in 7 different configurations. We chose  $r = 4$  as it worked best for the original configuration with all three features. The results are given in Table 2. Generally, the impact of the specific feature is low as the results vary by only  $\leq 0,3\%$ , indicating that all three features are good channel descriptors. The combinations involving GEP as well as the CATLite module with only GEP result in the best performance.

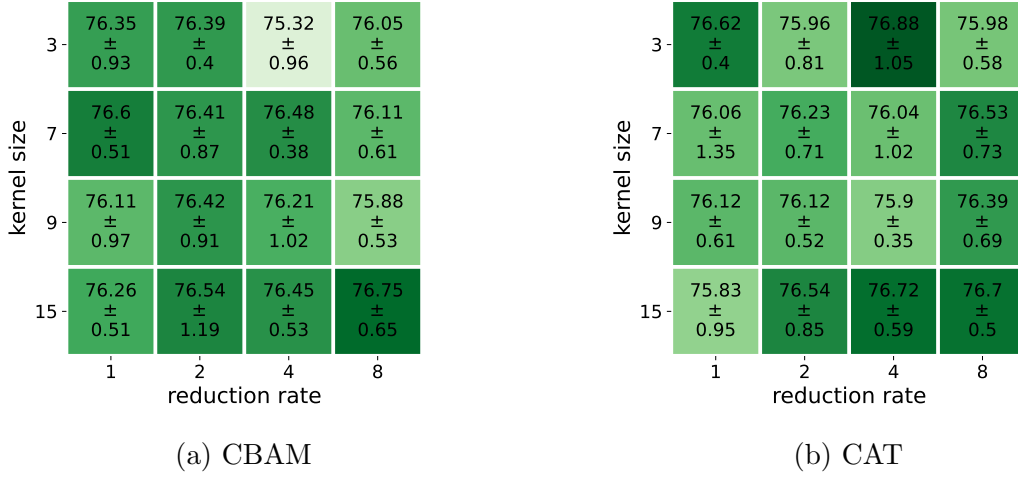


Figure 4: Ablation studies investigating the relationship between the reduction rate  $r$  in the channel attention module and the kernel size  $k$  in the temporal attention module.

### 3.3. Comparison with state of the art approaches

We also compared our models with four state-of-the-art approaches for the same EEG motor imagery decoding task and achieved better results than three of them, see Table 1. We included a lightweight architecture without attention (EEGTCNet), a model using the SE block (TS-SEFFNet) and two different approaches of using MHSA in the temporal domain to cover as many research directions as possible. For EEGTCNet we used only a 4s window instead of the reported 4.5s window and the ELU activation function instead of ReLU, as it showed better results than their reported configuration. Apart from that, we used the same learning rate scheduler as in our experiments for TS-SEFFNet, EEGConformer and EEGTCNet as it also improved the results. All other hyperparameters were kept identical to the reported ones. It is worth noting that we train the EEGConformer twice as long (2000 epochs) and with their data augmentation method (segmentation and reconstruction) because the authors originally also trained the model like that.

The performance of our simple BaseNet is above and at the level of more sophisticated approaches like TS-SEFFNet and EEGTCNet, respectively. Our best channel attention mechanisms outperform EEGConformer and EEGTCNet. ATCNet has the best overall decoding performance.

### 3.4. Transferability to other datasets

To investigate how our previous results transfer to other datasets, we evaluated the best models from Table 1 with exactly the same configuration on the BCI competition 2b and the High Gamma dataset. The results are presented in Table 3. For the 2b dataset, BaseNet with and without an additional attention mechanisms reaches around 84,5% performance, clearly outperforming EEGNet and ShallowNet. Between the attention

Table 3: Results of the best models from Table 1. The configurations are identical to the previous experiments.

model	BCIC 2b test acc. (%)	HGD test acc. (%)
EEGNet	83, 54 $\pm$ 0, 46	84, 68 $\pm$ 0, 91
ShallowNet	78, 41 $\pm$ 0, 99	88, 72 $\pm$ 0, 85
BaseNet	84, 34 $\pm$ 0, 36	93, 94 $\pm$ 0, 44
BaseNet + SE	84, 54 $\pm$ 0, 22	93, 48 $\pm$ 0, 38
BaseNet + ECANet	84, 14 $\pm$ 0, 4	93, 59 $\pm$ 0, 9
BaseNet + SRM	<b>84, 84 <math>\pm</math> 0, 69</b>	93, 3 $\pm$ 0, 39
BaseNet + SRM <sub>cross</sub>	82, 87 $\pm$ 0, 72	93, 86 $\pm$ 0, 82
BaseNet + CAT	84, 49 $\pm$ 0, 37	<b>94, 22 <math>\pm</math> 0, 6</b>
BaseNet + CATLite	84, 65 $\pm$ 0, 49	93, 51 $\pm$ 0, 61
TS-SEFFNet [2]	83, 27 $\pm$ 0, 27	91, 99 $\pm$ 0, 52
EEGConformer [10]	81, 02 $\pm$ 0, 53	<b>95, 32 <math>\pm</math> 0, 4</b>
ATCNet [11]	<b>85, 52 <math>\pm</math> 0, 44</b>	92, 61 $\pm$ 0, 67
EEGTCNet [12]	<b>85, 51 <math>\pm</math> 0, 42</b>	92, 24 $\pm$ 1, 2

mechanisms there are only minor differences except for the SRM models. In contrast to the experiments with the 2a dataset the cross-channel version performs worse than the original channel-independent version. Out of the state of the art approaches, ATCNet and EEGTCNet showed the best results, slightly surpassing our models.

For the HGD, our models again clearly outperform EEGNet and ShallowNet. The margins between the different attention mechanisms are small and there are no significant improvements by using an additional attention mechanism. In comparison with the state of the art approaches, BaseNet outperforms three out of four methods with only EEGConformer yielding better results.

#### 4. Discussion

The results across all three datasets show that our proposed BaseNet is a very strong, yet lightweight, architecture that results in a good performance under different motor imagery decoding settings. The two strongest competitors EEGConformer and ATCNet produce the best results for the HGD and the BCI competition datasets respectively, at the cost of producing poor results on the other dataset. It is worth noting that ATCNet, which outperforms our approaches on both BCI competition datasets, does this by using a temporally stacked ensemble model with 30x more parameters than BaseNet+CATLite which leads to a 20x increase of training time (on a NVIDIA RTX A6000: 6h 15min vs. 18,5min for the 2a dataset). So the lightweight architectures proposed by us might be the better choice if computational resources matter. In addition, they have better generalization capability across different datasets.

The results of the channel attention mechanisms along with the ablations show that



while there is room for improvement, the improvements between the mechanisms and configurations are quite small compared to the differences due to major changes in the architecture (cf. Figure 2b). As we used the best configuration from the 2a dataset for the 2b dataset and the HGD, this configuration is suboptimal and we suppose that there is still some room for improvements. Larger improvements, however, can probably be achieved by tailoring the BaseNet architecture towards the datasets, e.g. by using more or less convolutional filters.

One surprising insight from our investigations is, that the channel-independent SRM performed better than the cross-channel counterpart on the 2b dataset with only three sensors. On the 2a dataset with 22 sensors and the HGD with 44 sensors, however, the cross-channel version yields better results. This result indicates that the importance of cross-channel interaction depends on the number of sensors.

Using temporal and channel attention together, as in CBAM and CAT, resulted in good but not superior performance, suggesting that channel attention alone is sufficient and the combination with temporal attention is not necessary.

## **5. Conclusion**

We developed a simple and lightweight yet powerful framework for EEG motor imagery decoding which clearly outperforms the standard deep learning models EEGNet and ShallowNet on three datasets. Further, it performs very well across all three datasets compared to more sophisticated, computationally demanding state of the art approaches. Additionally, we systematically investigated and compared a wide range of channel attention mechanisms which can be integrated seamlessly into our BaseNet while maintaining a low complexity and a small memory footprint. The results show that additional channel attention can further improve the performance of the proposed BaseNet.

## **Acknowledgments**

This paper has been generated within the BMBF-funded Quantum Human Machine Interfaces (QHMI) project, a component of the QSens - Quantum Sensors of the Future cluster. We gratefully acknowledge the financial support provided by the BMBF, which was instrumental in advancing our research efforts. We also extend our deepest appreciation to our dedicated project partners, whose collaborative efforts were indispensable to the accomplishment of this study.

## **Conflict of Interest Statement**

The authors declare that the research was conducted in the absence of any commercial or financial relationships that could be construed as a potential conflict of interest.

## References

- [1] C. Liu, J. Jin, I. Daly, S. Li, H. Sun, Y. Huang, X. Wang, and A. Cichocki, "Sincnet-based hybrid neural network for motor imagery EEG decoding," *IEEE Transactions on Neural Systems and Rehabilitation Engineering*, vol. 30, pp. 540–549, 2022.
- [2] Y. Li, L. Guo, Y. Liu, J. Liu, and F. Meng, "A temporal-spectral-based squeeze-and-excitation feature fusion network for motor imagery EEG decoding," *IEEE Transactions on Neural Systems and Rehabilitation Engineering*, vol. 29, pp. 1534–1545, 2021.
- [3] G. A. Altuwaijri, G. Muhammad, H. Altaheri, and M. Alsulaiman, "A multi-branch convolutional neural network with squeeze-and-excitation attention blocks for EEG-based motor imagery signals classification," *Diagnostics*, vol. 12, no. 4, p. 995, 2022.
- [4] Z. Jia, Y. Lin, J. Wang, K. Yang, T. Liu, and X. Zhang, "Mmcnn: A multi-branch multi-scale convolutional neural network for motor imagery classification," in *Machine Learning and Knowledge Discovery in Databases: European Conference, ECML PKDD 2020, Ghent, Belgium, September 14–18, 2020, Proceedings, Part III*, pp. 736–751, Springer, 2021.
- [5] H. Zhang, X. Zhao, Z. Wu, B. Sun, and T. Li, "Motor imagery recognition with automatic EEG channel selection and deep learning," *Journal of Neural Engineering*, vol. 18, no. 1, p. 016004, 2021.
- [6] B. Sun, X. Zhao, H. Zhang, R. Bai, and T. Li, "EEG motor imagery classification with sparse spectrotemporal decomposition and deep learning," *IEEE Transactions on Automation Science and Engineering*, vol. 18, no. 2, pp. 541–551, 2020.
- [7] C. Szegedy, S. Ioffe, V. Vanhoucke, and A. Alemi, "Inception-v4, inception-resnet and the impact of residual connections on learning," in *Proceedings of the AAAI conference on artificial intelligence*, vol. 31, 2017.
- [8] K. He, X. Zhang, S. Ren, and J. Sun, "Identity mappings in deep residual networks," in *Computer Vision—ECCV 2016: 14th European Conference, Amsterdam, The Netherlands, October 11–14, 2016, Proceedings, Part IV 14*, pp. 630–645, Springer, 2016.
- [9] S. U. Amin, H. Altaheri, G. Muhammad, M. Alsulaiman, and W. Abdul, "Attention based inception model for robust EEG motor imagery classification," in *2021 IEEE international instrumentation and measurement technology conference (I2MTC)*, pp. 1–6, IEEE, 2021.
- [10] Y. Song, Q. Zheng, B. Liu, and X. Gao, "EEG Conformer: Convolutional transformer for EEG decoding and visualization," *IEEE Transactions on Neural Systems and Rehabilitation Engineering*, vol. 31, pp. 710–719, 2022.
- [11] H. Altaheri, G. Muhammad, and M. Alsulaiman, "Physics-informed attention temporal convolutional network for EEG-based motor imagery classification," *IEEE Transactions on Industrial Informatics*, vol. 19, no. 2, pp. 2249–2258, 2022.
- [12] T. M. Ingolfsson, M. Hersche, X. Wang, N. Kobayashi, L. Cavigelli, and L. Benini, "EEG-TCNet: An accurate temporal convolutional network for embedded motor-imagery brain-machine interfaces," in *2020 IEEE International Conference on Systems, Man, and Cybernetics (SMC)*, pp. 2958–2965, IEEE, 2020.
- [13] D. Zhang, K. Chen, D. Jian, and L. Yao, "Motor imagery classification via temporal attention cues of graph embedded EEG signals," *IEEE journal of biomedical and health informatics*, vol. 24, no. 9, pp. 2570–2579, 2020.
- [14] X. Ma, S. Qiu, and H. He, "Time-distributed attention network for EEG-based motor imagery decoding from the same limb," *IEEE Transactions on Neural Systems and Rehabilitation Engineering*, vol. 30, pp. 496–508, 2022.
- [15] Z. Miao, M. Zhao, X. Zhang, and D. Ming, "Lmda-net: A lightweight multi-dimensional attention network for general EEG-based brain-computer interfaces and interpretability," *NeuroImage*, p. 120209, 2023.
- [16] X. Liu, R. Shi, Q. Hui, S. Xu, S. Wang, R. Na, Y. Sun, W. Ding, D. Zheng, and X. Chen, "Tcacnet: Temporal and channel attention convolutional network for motor imagery classification of EEG-

- based bci,” *Information Processing & Management*, vol. 59, no. 5, p. 103001, 2022.
- [17] W. Tao, C. Li, R. Song, J. Cheng, Y. Liu, F. Wan, and X. Chen, “EEG-based emotion recognition via channel-wise attention and self attention,” *IEEE Transactions on Affective Computing*, 2020.
  - [18] A. Vaswani, N. Shazeer, N. Parmar, J. Uszkoreit, L. Jones, A. N. Gomez, L. Kaiser, and I. Polosukhin, “Attention is all you need,” *Advances in neural information processing systems*, vol. 30, 2017.
  - [19] R. T. Schirrmeister, J. T. Springenberg, L. D. J. Fiederer, M. Glasstetter, K. Eggensperger, M. Tangermann, F. Hutter, W. Burgard, and T. Ball, “Deep learning with convolutional neural networks for EEG decoding and visualization,” *Human brain mapping*, vol. 38, no. 11, pp. 5391–5420, 2017.
  - [20] V. J. Lawhern, A. J. Solon, N. R. Waytowich, S. M. Gordon, C. P. Hung, and B. J. Lance, “EEGNet: A compact convolutional neural network for EEG-based brain-computer interfaces,” *Journal of neural engineering*, vol. 15, no. 5, p. 056013, 2018.
  - [21] Q. Wang, B. Wu, P. Zhu, P. Li, W. Zuo, and Q. Hu, “Eca-net: Efficient channel attention for deep convolutional neural networks,” in *Proceedings of the IEEE/CVF conference on computer vision and pattern recognition*, pp. 11534–11542, 2020.
  - [22] B. Blankertz, R. Tomioka, S. Lemm, M. Kawanabe, and K.-R. Muller, “Optimizing spatial filters for robust EEG single-trial analysis,” *IEEE Signal processing magazine*, vol. 25, no. 1, pp. 41–56, 2007.
  - [23] K. K. Ang, Z. Y. Chin, H. Zhang, and C. Guan, “Filter bank common spatial pattern (FBCSP) in brain-computer interface,” in *2008 IEEE international joint conference on neural networks (IEEE world congress on computational intelligence)*, pp. 2390–2397, IEEE, 2008.
  - [24] A. Paszke, S. Gross, F. Massa, A. Lerer, J. Bradbury, G. Chanan, T. Killeen, Z. Lin, N. Gimelshein, L. Antiga, A. Desmaison, A. Kopf, E. Yang, Z. DeVito, M. Raison, A. Tejani, S. Chilamkurthy, B. Steiner, L. Fang, J. Bai, and S. Chintala, “PyTorch: An Imperative Style, High-Performance Deep Learning Library,” in *Advances in Neural Information Processing Systems 32* (H. Wallach, H. Larochelle, A. Beygelzimer, F. d’Alché Buc, E. Fox, and R. Garnett, eds.), pp. 8024–8035, Curran Associates, Inc., 2019.
  - [25] W. Falcon and The PyTorch Lightning team, “PyTorch Lightning,” Mar. 2019.
  - [26] A. Gramfort, M. Luessi, E. Larson, D. A. Engemann, D. Strohmeier, C. Brodbeck, R. Goj, M. Jas, T. Brooks, L. Parkkonen, *et al.*, “Meg and eeg data analysis with mne-python,” *Frontiers in neuroscience*, p. 267, 2013.
  - [27] V. Jayaram and A. Barachant, “Moabb: trustworthy algorithm benchmarking for bcis,” *Journal of neural engineering*, vol. 15, no. 6, p. 066011, 2018.
  - [28] C. Brunner, R. Leeb, G. Müller-Putz, A. Schlögl, and G. Pfurtscheller, “Bci competition 2008–graz data set a,” *Institute for Knowledge Discovery (Laboratory of Brain-Computer Interfaces), Graz University of Technology*, vol. 16, pp. 1–6, 2008.
  - [29] R. Leeb, C. Brunner, G. Müller-Putz, A. Schlögl, and G. Pfurtscheller, “Bci competition 2008–graz data set b,” *Graz University of Technology, Austria*, vol. 16, pp. 1–6, 2008.
  - [30] M.-H. Guo, T.-X. Xu, J.-J. Liu, Z.-N. Liu, P.-T. Jiang, T.-J. Mu, S.-H. Zhang, R. R. Martin, M.-M. Cheng, and S.-M. Hu, “Attention mechanisms in computer vision: A survey,” *Computational visual media*, vol. 8, no. 3, pp. 331–368, 2022.
  - [31] J. Hu, L. Shen, and G. Sun, “Squeeze-and-excitation networks,” in *Proceedings of the IEEE conference on computer vision and pattern recognition*, pp. 7132–7141, 2018.
  - [32] Z. Gao, J. Xie, Q. Wang, and P. Li, “Global second-order pooling convolutional networks,” in *Proceedings of the IEEE/CVF Conference on computer vision and pattern recognition*, pp. 3024–3033, 2019.
  - [33] Z. Qin, P. Zhang, F. Wu, and X. Li, “Fcanet: Frequency channel attention networks,” in *Proceedings of the IEEE/CVF international conference on computer vision*, pp. 783–792, 2021.
  - [34] H. Zhang, K. Dana, J. Shi, Z. Zhang, X. Wang, A. Tyagi, and A. Agrawal, “Context encoding for semantic segmentation,” in *Proceedings of the IEEE conference on Computer Vision and*

- Pattern Recognition*, pp. 7151–7160, 2018.
- [35] J. Hu, L. Shen, S. Albanie, G. Sun, and A. Vedaldi, “Gather-excite: Exploiting feature context in convolutional neural networks,” *Advances in neural information processing systems*, vol. 31, 2018.
  - [36] Z. Yang, L. Zhu, Y. Wu, and Y. Yang, “Gated channel transformation for visual recognition,” in *Proceedings of the IEEE/CVF conference on computer vision and pattern recognition*, pp. 11794–11803, 2020.
  - [37] H. Lee, H.-E. Kim, and H. Nam, “Srm: A style-based recalibration module for convolutional neural networks,” in *Proceedings of the IEEE/CVF International conference on computer vision*, pp. 1854–1862, 2019.
  - [38] S. Woo, J. Park, J.-Y. Lee, and I. S. Kweon, “Cbam: Convolutional block attention module,” in *Proceedings of the European conference on computer vision (ECCV)*, pp. 3–19, 2018.
  - [39] Z. Wu, M. Wang, W. Sun, Y. Li, T. Xu, F. Wang, and K. Huang, “Cat: Learning to collaborate channel and spatial attention from multi-information fusion,” *IET Computer Vision*, vol. 17, no. 3, pp. 309–318, 2023.
  - [40] D. P. Kingma and J. Ba, “Adam: A method for stochastic optimization,” *arXiv preprint arXiv:1412.6980*, 2014.